Bilayer membranes of triple-chain, fluorocarbon amphiphiles

Toyoki Kunitake, and Nobuyuki Higashi

J. Am. Chem. Soc., **1985**, 107 (3), 692-696• DOI: 10.1021/ja00289a025 • Publication Date (Web): 01 May 2002

Bilayer Membranes of Triple-Chain, Fluorocarbon Amphiphiles

Toyoki Kunitake* and Nobuyuki Higashi

Contribution No. 728 from the Department of Organic Synthesis, Faculty of Engineering, Kyushu University, Fukuoka, 812 Japan. *Received June 18, 1984*

Abstract: Triple-chain ammonium amphiphiles were prepared in which one, two, or three fluorocarbon chains are present. They formed clear aqueous dispersions upon sonication. Electron microscopy indicated the formation of bilayer vesicles. Differential scanning calorimetry (DSC) and fluorescence depolarization experiments (probes: anilinonaphthalenesulfonate and diphenylhexatriene) established the presence of crystal-to-liquid crystal transitions in all cases: 36–54 °C. The fluidity of the liquid-crystalline bilayers near the membrane surface *increased* with increasing numbers of the fluorocarbon tail, whereas that of the bulk membrane *decreased* with increasing fluorocarbon tails. Mixing behavior of bilayers was examined by DSC. The totally fluorocarbon-tailed bilayer did not readily mix with totally or partially hydrocarbon-tailed bilayers. In contrast, the totally hydrocarbon-tailed bilayer mixed more readily with partially fluorocarbon-tailed bilayers. Finally, the use of the present bilayer system for constructing complex molecular assemblies was discussed.

We have shown in a previous paper[1] that stable bilayer assemblies are formed from series of triple-chain ammonium amphiphiles. The physicochemical characteristics of these bilayers are basically similar to those of the aqueous bilayer obtained from single- and double-chain amphiphiles. These findings establish that bilayer formation is a widely observable phenomenon among several types of synthetic amphiphiles.

Fluorocarbon amphiphiles display aggregation characteristics which are often quite distinct from those of the hydrocarbon counterpart. The limited miscibility of fluorocarbon and hydrocarbon amphiphiles[2-6] has been applied to selective micellar catalysis.[7,8] We reported recently that some single- and double-chain amphiphiles which possess fluorocarbon tails in place of hydrocarbon tails similarly undergo spontaneous bilayer assemblage.[9] Fluorocarbon bilayer vesicles possess enhanced barrier capabilities against ion permeation. It is also possible to control the extent of phase separation by taking advantage of limited miscibility of hydrocarbon and fluorocarbon components.[10]

In the present paper we wish to describe a new class of bilayer-forming amphiphiles. They are triple-chain ammonium amphiphiles in which one, two, or three of the long chains are fluorocarbon. These amphiphiles produce bilayer aggregates when dispersed in water, and the resulting bilayer membranes display peculiar properties. The new fluorocarbon amphiphiles are shown in Chart I, together with the related hydrocarbon amphiphiles.

Experimental Section

Materials. *O,O',O''*-Tris(2*H*,2*H*,3*H*,3*H*-perfluoroundecanoyl)-*N*-(ω-(trimethylammonio)undecanoyl)tris(hydroxymethyl)aminomethane Bromide ($3C_8^FC_3$-tris-$C_{11}N^+$). Tris(hydroxymethyl)aminomethane (3.6 g, 0.03 mol), 47.2 g (0.098 mol) of 2*H*,2*H*,3*H*,3*H*-perfluoroundecanoic acid (Ugine Kuhlmann), and 9.4 g (0.05 mol) of *p*-toluenesulfonic acid were dissolved in toluene, and the mixture was heated with magnetic stirring. The heating was continued until the theoretical amount of water was removed by a Dean-Stark trap. Then, toluene was removed in vacuo, and the residue was recrystallized from dimethylformamide (DMF).

Chart I

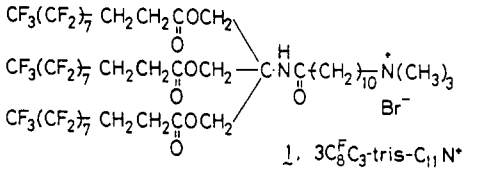

1, $3C_8^FC_3$-tris-$C_{11}N^+$

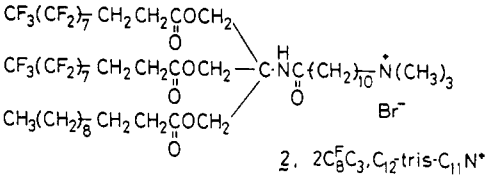

2, $2C_8^FC_3, C_{12}$-tris-$C_{11}N^+$

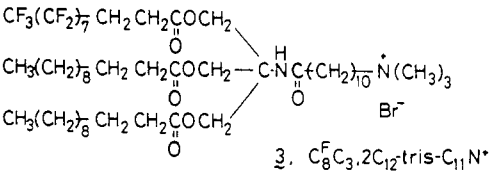

3, $C_8^FC_3, 2C_{12}$-tris-$C_{11}N^+$

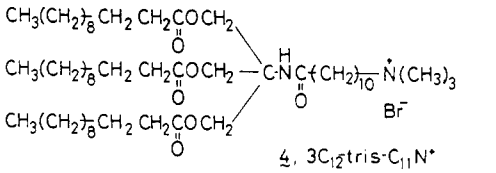

4, $3C_{12}$-tris-$C_{11}N^+$

Several washing by ethanol gave a pale brown solid: yield 32%, mp 173–175 °C; IR $\nu_{C=O}$ 1750 cm^{-1} (ester), ν_{CF} 1100–1300 cm^{-1}, ν_{OH} absent; NMR ($CDCl_3$, triethylamine) δ 4.32 (s, 6, OCH_2), 7.20 (d) and 7.75 (d) (4, phenyl).

The triester tosylate obtained (2.2 g, 0.013 mol) and 1 mL of triethylamine were dissolved in a 5:1 (by volume) mixture of dry tetrahydrofuran (THF) and 1,1,2-trifluoro-1,2,2-trichloroethane (Fronsolve), and 0.43 g (0.0015 mol) of 11-bromoundecanoyl chloride in dry THF was added dropwise in 20 min to the stirred reaction mixture in an ice bath. The mixture was additionally stirred for 24 h at room temperature and the precipitate of triethylamine hydrochloride was removed. After solvent removal, the solid residue was recrystallized from a 10:1 mixture of ethanol and ethyl acetate, giving pale yellow powders in 77% yield. Quaternization of the product was conducted in 1:1 THF–benzene for 3 days with a large excess of trimethylamine. The precipitates produced upon ice cooling were recrystallized from ethyl acetate to give pale brown powders of **1** in 65% yield, mp 41 → 68 °C (the arrow indicates the liquid-crystalline range). Anal. Calcd for $C_{51}H_{38}O_7N_2F_{51}Br\cdot 2H_2O$: C, 32.66; H, 2.26; N, 1.49. Found: C, 32.57; H, 2.49; N, 1.45. IR $\nu_{C=O}$

(1) Kunitake, T.; Kimizuka, N.; Higashi, N.; Nakashima, N. *J. Am. Chem. Soc.* **1984**, *106*, 1978–1983.
(2) Mukerjee, P.; Yang, A. Y. S. *J. Phys. Chem.* **1976**, *80*, 1388–1390.
(3) Mysels, K. J. *J. Colloid Interface Sci.* **1978**, *66*, 331–334.
(4) Mukerjee, P.; Mysels, K. J. *ACS Symp. Ser.* **1975**, *No. 9*. 239–252.
(5) Funasaki, N.; Hada, S. *Chem. Lett.* **1979**, 717–718; *J. Phys. Chem.* **1980**, *84*, 736–744.
(6) Shinoda, K.; Nomura, T. *J. Phys. Chem.* **1980**, *84*, 365–369.
(7) Ihara, H.; Hashiguchi, Y.; Kunitake, T. *Chem. Lett.* **1983**, 733–736.
(8) Kunitake, T.; Ihara, H.; Hashiguchi, Y. *J. Am. Chem. Soc.* **1984**, *106*, 1156–1157.
(9) Kunitake, T.; Okahata, Y. Yasunami, S. *J. Am. Chem. Soc.* **1982**, *104*, 5547–5549.
(10) Kunitake, T.; Tawaki, S.; Nakashima, N. *Bull. Chem. Soc. Jpn.* **1983**, *56*, 3235–3242.

0002-7863/85/1507-0692$01.50/0

1745 cm^{-1} (ester), $\nu_{C=O}$ 1640 cm^{-1} (amide); NMR ($CDCl_3$) δ 3.40 (s, 9, N^+CH_3), 4.45 (s, 6, OCH_2).

***O,O'*-Di(2*H*,2*H*,3*H*,3*H*-perfluoroundecanoyl)-*O''*-dodecanoyl-*N*-(ω-(trimethylammonio)undecanoyl)tris(hydroxymethyl)aminomethane Bromide ($2C_8^FC_3$,C_{12}-tris-$C_{11}N^+$, 2).** Tris(hyroxylmethyl)aminomethane (2.4 g, 0.02 mol), 4.1 g (0.02 mol) of dodecanoic acid, and 5.4 g (0.028 mol) of *p*-toluensulfonic acid were dissolved in toluene and allowed to react as described above. Upon standing overnight, the precipitates formed were recrystallized from a 5:1 mixture of acetone and methanol to give colorless needles in 47% yield: mp 51–52 °C; IR $\nu_{C=O}$ 1745 cm^{-1} (ester), ν_{OH} 3360 cm^{-1}; NMR (Me_2SO-d_6) δ 3.57 (s, 4, HO-CH_2), 4.12 (s, 2, O-CH_2), 7.15 (d) and 7.55 (d) (4, phenyl). The spectroscopic data indicated formation of the monoester.

The monoester (2 g, 0.0042 mol) was dissolved in toluene together with 4.9 g (0.010 mol) of 2*H*,2*H*,3*H*,3*H*-perfluoroundecanoic acid and 2,2 g (0.012 mol) of *p*-toluenesulfonic acid and allowed to undergo esterification as described above: pale brown powders from 3:1 DMF–ethanol, yield 25%: mp 150 → 165 °C; IR ν_{OH} absent, ν_{CF} 1100–1300 cm^{-1}; NMR ($CDCl_3$) δ 4.46 (s, 6, OCH_2), 7.20 (d) and 7.82 (d) (4, phenyl). The triester obtained (4.0 g, 0.0028 mol) and 1 mL of triethylamine were dissolved in a 5:1 mixture of dry THF and Fronsolve, and 2.0 g (0.007 mol) of 11-bromoundecanoyl chloride in dry THF was added dropwise with ice cooling. After stirring for 24 h at room temperature, triethylamine hydrochloride was removed and the solvent was evaporated. Recrystallization of the residue from 10:1 ethanol–ethyl acetate gave pale brown powders in 72% yield, IR $\nu_{C=O}$ (amide) 1670 cm^{-1}. Quaternization with trimethylamine was conducted as described above, and the product was recrystallized from 50:1 ethyl acetate–ethanol to give colorless powders in 62% yield, mp 62 → 148 °C. Anal. Calcd for $C_{52}H_{67}O_7N_2F_{34}Br{\cdot}H_2O$: C, 39.63; H, 4.29; N, 1.78. Found: C, 39.39; H, 4.20; N, 1.84.

***O*-(2*H*,2*H*,3*H*,3*H*-perfluoroundecanoyl)-*O'*,*O''*-didodecanoyl-*N*-(ω-(trimethylammonio)undecanoyl)tris(hydroxymethyl)aminomethane Bromide ($C_8^FC_3$,$2C_{12}$-tris-$C_{11}N^+$, 3).** Tris(hydroxymethyl)aminomethane (9.7 g, 0.08 mol), 10 g (0.02 mol) of 2*H*,2*H*,3*H*,3*H*-perfluoroundecanoic acid, and 24 g (0.13 mol) of *p*-toluenesulfonic acid were allowed to react in toluene as described above. Pale brown powders were obtained in 51% yield after cooling in a freezer and recrystallization from ethanol, mp 169–171 °C. The formation of the monoester was confirmed spectroscopically: IR $\nu_{C=O}$ 1740 cm^{-1} (ester), ν_{CF} 1100–1300 cm^{-1}, ν_{OH} 3320 cm^{-1}; NMR (CD_3OD) δ 3.60 (s, 4, $HOCH_2$), 4.32 (s, 2, OCH_2), 7.20 (d) and 7.68 (d) (4, phenyl).

The monoester (3 g, 0.004 mol), 2 g (0.011 mol) of dodecanoic acid, and 2 g (0.011 mol) of *p*-toluenesulfonic acid were allowed to react in toluene as described above, and the triester precipitates formed upon cooling were recrystallized from ethyl acetate; colorless powders, yield 31%, mp 130–134 °C, IR $\nu_{C=O}$ 1740 cm^{-1} (ester), ν_{OH} absent. The triester (1.1 g, 0.001 mol) in 5:1 dry THF–Fronsolve was allowed to react with 0.4 g (0.0014 mol) of 11-bromoundecanoyl chloride in dry THF as described above, and the product was recrystallized from 10:1 ethanol–ethyl acetate, colorless powders, yield 39%: mp room temperature → 43 °C, IR $\nu_{C=O}$ 1735 cm^{-1} (ester), $\nu_{C=O}$ 1680 cm^{-1} (amide). Quaternization with trimethylamine (in 1:1 THF–benzene, 3 days) and recrystallization from ethyl acetate gave colorless powders in 63% yield: mp 73–75 °C, NMR ($CDCl_3$) δ 3.45 (s, 9, N^+CH_3), 3.62 (s, 2, N^+CH_2), 4.42 (s, 6, OCH_2). Anal. Calcd for $C_{52}H_{90}O_7N_2F_{17}Br$: C, 46.68; H, 6.78; N, 2.09. Found: C, 46.86; H, 6.29; N, 2.12.

Measurements. Aqueous solutions of amphiphiles were prepared by sonication (Bransonic Sonifier 185, microtip, sonic power 40). The morphology of bilayer aggregates was observed by transmission electron microscopy (instrument, Hitachi H-600) as described before.[11] Differential scanning calorimetry (DSC) was conducted for 20-mM samples (instrument, Daini-Seikosha SSC/560). The temperature was raised at a rate of 2 °C/min from 0 °C.[12]

Fluorescence depolarization was examined for 1,6-diphenyl-1,3,5-hexatriene (DPH, Tokyo Kasei) and sodium-8-anilino-1-naphthalenesulfonate (ANS, Tokyo Kasei). The stock solutions (5 μL, 1×10^{-3} M) of these fluorescence probes (DPH in THF and ANS in water) were added to 5 mL of aqueous dispersions (1×10^{-3} M) of amphiphiles and sonicated. In the case of DPH probe, THF was removed before mixing. Emission spectra were measured with Hitachi 650-10S spectrofluorimeter, and the degree of polarization, *P*, was calculated by eq 1.

$$P = \frac{I_{\parallel\parallel} - I_{\parallel\perp}(I_{\perp\parallel}/I_{\perp\perp})}{I_{\parallel\parallel} + I_{\parallel\perp}(I_{\perp\parallel}/I_{\perp\perp})} \quad (1)$$

(11) Kunitake, T.; Okahata, Y. *J. Am. Chem. Soc.* **1980**, *102*, 549–553.
(12) Okahata, Y.; Ando, R.; Kunitake, T. *Ber. Bunsenges. Phys. Chem.* **1981**, *85*, 789–798.

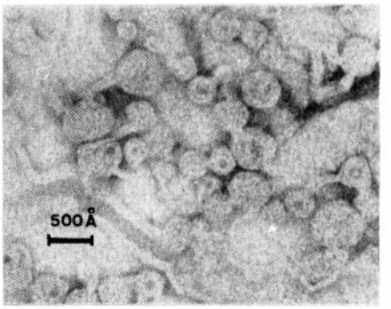

Figure 1. Electron micrograph of $3C_8^FC_3$-tris-$C_{11}N^+$, stained by uranyl acetate, original magnification × 40 000.

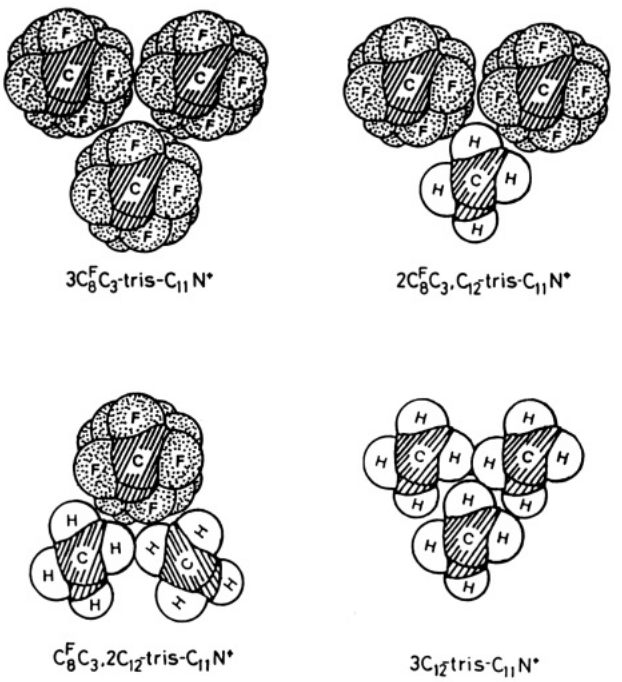

Figure 2. Molecular cross sections of triple-chain amphiphiles.

Table I. Phase-Transition Behavior

amphiphile (20 mM in water)	DSC endothermic peak, °C	DSC ΔH, kcal/mol	inflection points of *P* values (DPH), °C
$3C_8^FC_3$-tris-$C_{11}N^+$	53.7	1.4	51
$2C_8^FC_3$,C_{12}-tris-$C_{11}N^+$	46.0	2.1	46
$C_8^FC_3$,$2C_{12}$-tris-$C_{11}N^+$	36.1	5.0	37
$3C_{12}$-tris-$C_{11}N^+$	41.5	7.6	41

Results and Discussion

Aggregate Morphology. Clear solutions are obtainable when the triple-chain fluorocarbon amphiphiles (20 mM) are dispersed in water by sonication. Figure 1 shows an electron micrograph of the aqueous dispersion of $3C_8^FC_3$-tris-$C_{11}N^+$. Vesicles are found with layer thicknesses of 80–90 Å, which correspond approximately to two molecular lengths. Similar morphologies are found for other fluorocarbon amphiphiles. It is apparent that the fluorocarbon amphiphiles form bilayer assemblage spontaneously. The corresponding hydrocarbon amphiphile, $3C_{12}$-tris-$C_{11}N^+$, similarly produces bilayer vesicles.[1] These four amphiphiles are completely identical in the head group (trimethylammonium) and spacer (C_{11}) structures and almost identical in the tail length. Therefore, substitution of the fluorocarbon chain for the hydrocarbon chain does not affect the aggregate morphology detectably, although the molecular cross section of the tail portion differs considerably among them (Figure 2).

Phase Transition. The bilayer membrane of synthetic hydrocarbon amphiphiles usually displays the crystal–liquid crystal phase transition, as studied systematically for double-chain compounds.[12]

The phase transition has been detected most directly by differential scanning calorimetry (DSC). Table I summarizes the DSC results. The endothermic peak of $3C_{12}$-tris-$C_{11}N^+$ at 41.5 °C has been attributed to the phase transition.[1] The endothermic peak appears at a lower temperature (36 °C) when one of the hydrocarbon chain is replaced with a fluorocarbon chain, whereas introduction of two or three fluorocarbon chains shifts the peak to higher temperatures. The enthalphy change (ΔH) represented by the peak area decreases with increasing numbers of the fluorocarbon chain.

The major phase transition of the representative hydrocarbon bilayers is usually associated with conversion of the all-trans conformation of the alkyl chain to the conformation that contains the gauche structure.[13] It is not assured whether or not this mechanism is applicable to the DSC behavior of the fluorocarbon bilayer. Because of the short C–F bond length (1.317 Å) and the bulky van der Waals radius of fluorine (1.35 Å), the CF_2 chain assumes a stiff, helical conformation. These characteristics are typically illustrated by poly(tetrafluoroethylene).[14] Poly(tetrafluoroethylene) melts at 327 °C with an entropy change (ΔS) of 1.14 cal mol^{-1} deg^{-1}, while poly(ethylene) melts at 137.5 °C with ΔS = 2.34 cal mol^{-1} deg^{-1}. The glass transition temperature (Tg) of poly(tetrafluoroethylene) is 127 °C, and crystalline transitions (β transition) due to the torsional oscillation of the carbon–carbon bond are found at 19 ad 30 °C.[14,15] The unique thermal behavior of poly(tetrafluoroethyene) relative to that of poly(ethylene) suggests that the phase-transition mechanism of the fluorocarbon bilayers is not necessarily the same as that of the hydrocarbon bilayer. We assume at the moment that the DSC peak observed for $3C_8^FC_3$-tris-$C_{11}N^+$ bilayer is associated with melting of the spacer methylene. In the case of partially fluorocarbon-tailed amphiphiles, melting of the spacer methylene and the hydrocarbon tail would contribute to the DSC peak. The stiff fluorocarbon tail should become more mobile due to the transition.

The contribution of the spacer methylene to the DSC behavior is apparent in the case of related double-chain amphiphiles

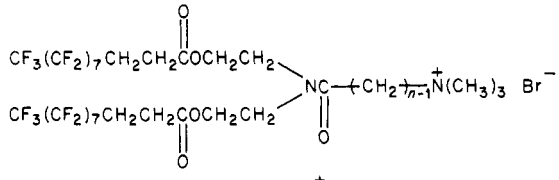

5, $2C_8^FC_3$-de-$C_n\overset{+}{N}$, n = 2, 6, 11

The fluorocarbon amphiphiles **5** produce bilayers.[16] These bilayers give rise to endothermic peaks. The phase transition shifts to lower temperatures from 75 to 71 to 53 °C, as the spacer methylene becomes longer from C_2 to C_6 to C_{11}, respectively. The enthalphy changes (ΔH) were 0.4–0.7 kcal/mol and were not affected by the spacer length. The melting of the spacer methylene must play a major role in the DSC behavior. It would not be an accidental coincidence that the bilayer membranes of double- and triple-chain fluorocarbon amphiphiles with the identical spacer length, $2C_8^FC_3$-de-$C_{11}N^+$ and $3C_8^FC_3$-tris-$C_{11}N^+$, give closely located DSC peaks (53.0 and 53.7 °C, respectively).

Membrane Fluidity. The nature of the phase transition can be elucidated by using fluorescence probes. Sodium 8-anilino-1-naphthalenesulfonate(ANS) has been used as a probe of the medium or the binding site, since its emission characteristics (maxium wavelength and intensity) change with the polarity of the environment: e.g., λ_{max} 515 nm in water and 468 nm in ethanol.[17] Emission maxima of ANS in the presence of the bilayer membrane of the four triple-chain amphiphiles are located at 480 nm and the intensities are much enhanced relative to that observed without the bilayer. These data are indicative of binding of ANS to the hydrophobic region near the bilayer surface, as would be expected for hydrophobic anions such as ANS. Apparently, the structural change in the tail (hydrocarbon vs. fluorocarbon) does not affect the microenvironment near the membrane surface.

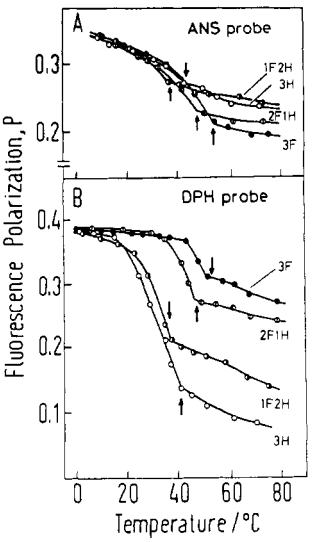

Figure 3. Temperature dependence of fluorescence polarization of ANS (A) and DPH (B) in bilayer matrices of triple-chain amphiphiles. [amphiphile] = 1×10^{-3} M, [probe] = 1×10^{-6} M. The arrow indicates the peak-top temperature in the DSC thermogram. The notations (3F, 2F1H, 1F2H, and 3H) indicate the number of hydrocarbon (H) and fluorocarbon (F) tails contained in a given amphiphile.

Fluoroescence depolarization is useful for evaluating the fluidity of the bilayer membrane.[18] Figure 3A demonstrates the temperature dependence of P for ANS fluorescence. At low temperatures, the P value is not affected by the kind of bilayer and gradually decreases with increasing temperature. There are breaks in the respective curves in the phase-transition region, and the curves are separated in the high-temperature region.

The magnitude of the P value represents the lack of fluidity of the environment around the probe molecule. Accordingly, the data of Figure 3A suggest that the fluidity near the surface is virtually the same in the crystalline bilayers, irrespective of the presence of the fluorocarbon chain. The fluidity changes discontinuously near T_c, which are indicated by the arrows, and the influence of the fluorocarbon tail become noticeable in the liquid-crystalline state. The $3C_8^FC_3$-tris-$C_{11}N^+$ bilayer possesses the surface region that is more fluid than that of the $2C_8^FC_3$,C_{12}-tris-$C_{11}N^+$ bilayer. The $C_8^FC_3$,$2C_{12}$-tris-$C_{11}N^+$ and $3C_{12}$-tris-$C_{11}N^+$ bilayers produces the least fluid surface region.

The change of the membrane fluidity can be estimated more clearly by using a second fluorescence probe, 1,6-diphenyl-1,3,5-hexatriene (DPH). This hydrophobic probe is believed to be buried deep in the bilayer matrix, and its P value is sensitive to the change in the molecular orientation.[18-19] Figure 3B illustrates the variation of P with temperature. The drop of the P value near T_c is more drastic in this case than that observed for ANS. The inflection temperatures (given in Table I) are very close to the respective peak temperatures in DSC. The pattern of the temperature dependence is quite similar to those observed for other bilayer systems,[1,20] and the coincidence of temperature convinces us that the endothermic peaks in DSC are indeed attributed to the commonly observed crystal-to-liquid crystal phase transition.

The P values in the high-temperature region are very different among the four bilayers. The increase in the membrane fluidity upon phase transition is largest for the totally hydrocarbon bilayer

(13) E.g.: Aloia, R. C., Ed. "Membrane Fluidity in Biology"; Academic Press: New York, 1983; Vol. 2.
(14) McCrum, N. G. *J. Polym. Sci.* **1958**, *27*, 555–597; **1959**, *34*, 355–369.
(15) Natarajan, R.; Davidson, T. *J. Polymer Sci. Polym. Phys. Ed.* **1972**, *10*, 2209–2222.
(16) Asakuma, S., unpublished results in these laboratories.
(17) Stryer, L. *J. Mol. Biol.* **1965**, *13*, 482–495.
(18) Shinitzky, M.; Barenholz, Y. *Biochim. Biophys. Acta* **1978**, *515*, 367–394.
(19) Shinitzky, M.; Barenholz, Y. *J. Biol. Chem.* **1974**, *249*, 2652–2657.
(20) Nagamura, T.; Mihara, S.; Okahata, Y.; Kunitake, T.; Matsuo, T. *Ber. Bunsenges. Phys. Chem.* **1978**, *82*, 1093–1098.

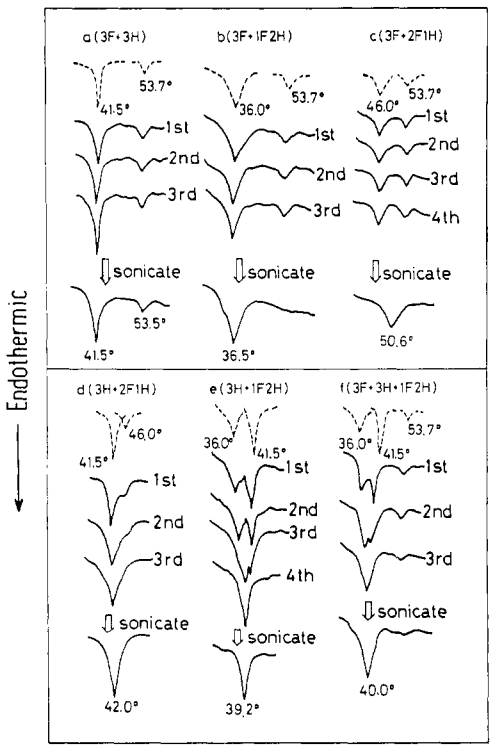

Figure 4. DSC thermograms of triple-chain amphiphiles. Dotted line: single-component bilayers, 20 mM. Solid line: multicomponent bilayers, 20 mM each. (a) 3F + 3H (see Figure 3 for the notation), (b) 3F + 1F2H, (c) 3F + 2F1H, (d) 3H + 2F1H, (e) 3H + 1F2H, (f) 3F + 3H + 1F2H.

($3C_{12}$-tris-$C_{11}N^+$), and the extent of the increase (lowering of P) diminishes with increasing fluorocarbon chains. The bilayer matrix (hydrophobic region) does not become highly fluid even after phase transition, when the rigid fluorocarbon chain is present.

Membrane Mixing. Fluorocarbons are not readily miscible with hydrocarbons. This property has been used to control phase separation of the bilayer membrane of double-chain, fluorocarbon amphiphiles with the corresponding hydrocarbon bilayer.[10] The mixing characteristics of triple-chain amphiphiles would be particularly interesting, since the number of the fluorocarbon chain can be changed from zero to three. DSC thermograms of single-component and multicomponent bilayers are shown in Figure 4. The dotted lines represent thermograms of the individual bialyers and the solid lines are thermograms of mixed bilayers. Figure 4a shows the DSC behavior of an equimolar mixture of $3C_8^FC_3$-tris-$C_{11}N^+$ and $3C_{12}$-tris-$C_{11}N^+$. This thermogram is the same as the sum of the individual thermograms after repeated scans or even after sonication. Therefore, these two bilayers are almost completely immiscible. In the case of a mixture of $3C_8^FC_3$-tris-$C_{11}N^+$ and $C_8^FC_3,2C_{12}$-tris-$C_{11}N^+$ (Figure 4b), the two components are not miscible by repeated scans, but the peak of $3C_8^FC_3$-tris-$C_{11}N^+$ disappears after sonication. A similar situation arises for the combination of $3C_8^FC_3$-tris-$C_{11}N$ and $2C_8^FC_3,C_{12}$-tris-$C_{11}N^+$, although the new peak appears at an intermediate temperature (Figure 4c). It is concluded that totally fluorocarbon-tailed bilayer of $3C_8^FC_3$-tris-$C_{11}N^+$ does not readily mix with totally or partially hydrocarbon-tailed bilayers.

On the other hand, the hydrocarbon bilayer of $3C_{12}$-tris-$C_{11}N^+$ mixes more readily with the bilayers of partial fluorocarbon tails ($2C_8^FC_3,C_{12}$-tris-$C_{11}N^+$ and $C_8^FC_3,2C_{12}$-tris-$C_{11}N^+$). The two separate peaks merge into one after several scans, as shown in Figure 4, parts d and e.

The two immiscible bilayers can be made miscible by introducing a third component that is separately miscible with either of the original components. Figure 4f is the thermogram of an equimolar mixture of $3C_8^FC_3$-tris-$C_{11}N^+$, $3C_{12}$-tris-$C_{11}N^+$, and $C_8^FC_3,2C_{12}$-tris-$C_{11}N^+$. The first two components are not miscible with each other as shown in Figure 4a, but the third component is miscible with the first and second components (Figure 4, parts b and e). After repeated scans, $3C_{12}$-tris-$C_{11}N^+$ and $C_8^FC_3,2C_{12}$-tris-$C_{11}N^+$ becomes mixed but the peak of $3C_8^FC_3$-tris-$C_{11}N^+$ remains. This peak is made much broader by sonication. It appears that some amount of the $3C_8^FC_3$-tris-$C_{11}N^+$ cluster is maintained at this molar ratio. These situations are visualized in Figure 5.

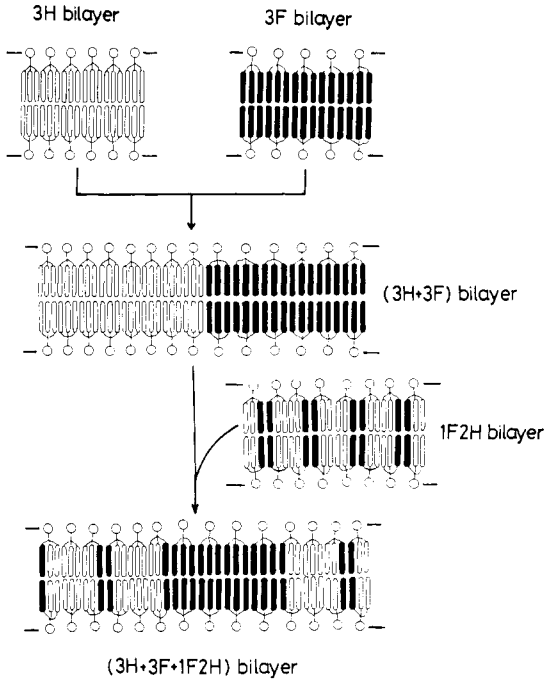

Figure 5. Schematic illustrations of the mixing in multicomponent bilayers.

It is interesting to compare this miscibility property with that of the bilayer of related double-chain amphiphiles. In a previous study,[10] we prepared aqueous bilayer membranes of $2C_8^FC_3$-de-N^+(**6**), $C_8^FC_3,C_{12}$-de-N^+(**7**), and $2C_{12}$-de-N^+(**8**). When equimolar

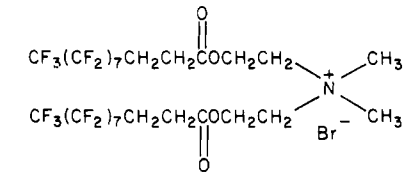

6, $2C_8^FC_3$-de-N^+

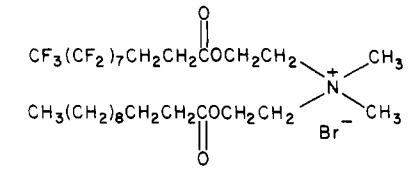

7, $C_8^FC_3, C_{12}$-de-N^+

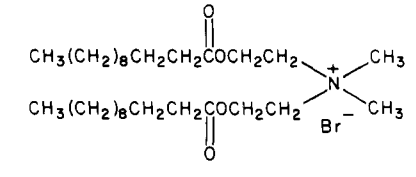

8, $2C_{12}$-de-N^+

amounts of the fluorocarbon bilayer **6** and the hydrocarbon bilayer **8** are mixed, the DSC pattern indicates the formation of partially miscible membranes. Addition of equimolar $C_8^FC_3,C_{12}$-de-N^+ as a third component causes disappearance of all the DSC peaks, suggesting random mixing in the three-component system. The partially fluorocarbon-tailed amphiphile is quite effective as a homogenizer of the totally hydrocarbon and totally fluorocarbon bilayers, in the case of double-chain amphiphiles.

Concluding Remarks

Triple-chain ammonium amphiphiles that contain fluorocarbon chains were shown to undergo spontaneous bilayer assemblage in water. The phase-transition behavior and the membrane fluidity are strongly affected by the number of the fluorocarbon tail. The phase-separation behavior is largely determined by the number of the fluorocarbon tail in an amphiphile. The controllable miscibility and the different molecular cross sections displayed in Figure 2 give us expectation that a large variety of new molecular assemblages can be designed. For instance, the distance between the surface polar groups may be controlled by using different sets of the tail. Two-dimensional distributions of particular functional groups may also be designed by taking advantage of limited component miscibility.

Acknowledgment. We extend our appreciation for financial support to Special Coordination Funds for Promoting Science and Technology from Science and Technology Agency of Japan.

Communications to the Editor

Chain Growth Rates in Fischer–Tropsch Synthesis on an Iron Catalyst: An Isotopic Transient Study

C. A. Mims* and L. E. McCandlish

Exxon Research and Engineering Company
Corporate Research Laboratories
Annandale, New Jersey 08801
Received October 9, 1984

We have examined the Fischer–Tropsch reaction by following both the rate and position of incorporation of ^{13}C into C_4 hydrocarbons after exchanging ^{13}CO for ^{12}CO in the reactant gas. Such isotopic transients under reaction steady state provide a valuable tool for the in situ study of catalytic reactions. The formation of CH_4 from CO and H_2 has been extensively studied by this technique,[1-4] and Biloen[2] has previously placed a lower bound on C–C bond formation rates by measuring the appearance rate of a new carbon isotope in C_3 fragments.

By examining *both* the rate and position of new label incorporation we are able to show that the major fraction of the hydrocarbon product at steady state derives from a much smaller number of growing chains than previously thought. Our data also place a lower limit to the average rate of chain growth in this system of two to four bonds per second.

The reaction was carried out in a small fixed bed reactor on 650 mg of promoted iron catalyst prepared in a manner similar to Dry's.[5] Table I lists the experimental conditions which were chosen to maximize selectivity to terminal olefins. We determined the molecular distribution of the ingrowing label by GC/MS analysis[6] of portions of the product gas sampled at selected times after the switch from ^{12}CO to ^{13}CO. NMR analysis of the intermediately labeled product revealed the location of the new label within the product molecules.

The evolution of the isotopic composition of the butene product is shown in Figure 1. A distribution of exchange rates for surface carbon is needed to describe the transient in Figure 1f, a fact consistent with previous reports by Biloen[2] and Bell.[4] Determination of the total amount of "active" surface carbon is hampered by difficulty in integrating the long tail in the transient. Integration of the transient in Figure 1f to the point of 90% isotopic exchange shows that a small amount (<1 μmol of C/g of catalyst) of surface carbon is responsible for 90% of the steady-state butene product. A more complete discussion of the transient kinetic behavior will be the subject of a separate paper.

Table I

temp, K	510
H_2/CO ratio	1.0
total pressure, kPa	90
gas residence time, s	0.15
catalyst surface area (freshly reduced), $m^2\ g^{-1}$	~40
productivity, nmol s^{-1} (g of cat.)$^{-1}$	
C2	8.6
C3	6.7
C4	4.8
C5	3.3
C6	2.3
olefin/paraffin	>10

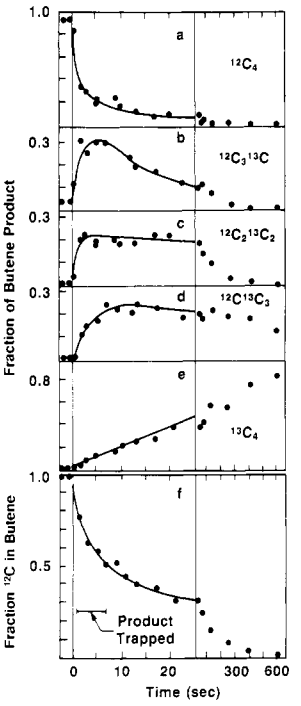

Figure 1. Evolution of ^{13}C into butene product after switch from ^{12}CO to ^{13}CO in reactant gas. (a–e) Distribution of the butene product among the isotopic variants $^{12}C_x{}^{13}C_{4-x}$. Note the change of time scale at 25 s. (f) The amount of ^{12}C in the butene product obtained by combination of data in (a–e). Product for NMR analysis was collected during the interval marked by the horizontal bar.

The positional distribution of ^{13}C was determined by proton NMR analysis of transiently labeled product collected in the 6-s interval indicated in Figure 1.[7] The collected product contains

(1) Happel, J.; Suzuki, I.; Kokayeff, P.; Fthenakis, V. *J. Catal.* **1980**, *65*, 59. Happel, J.; et al. *J. Catal.* **1982**, *75*, 314. Otarod, M.; et al. *J. Catal.* **1983**, *84*, 156.
(2) Biloen, P.; Helle, J. N.; van den Berg, F. G. A.; and Sachtler, W. M. H. *J. Catal.* **1983**, *81*, 450.
(3) Kobori, Y.; Yamasaki, H.; Naito, S.; Onishi, T.; Tamaru, K. *J. Chem. Soc., Faraday Trans. 1* **1982**, *78*, 1473.
(4) Cant, N. W.; Bell, A. T. *J. Catal.* **1982**, *73*, 257. Winslow, P.; Bell, A. T. *J. Catal.* **1984**, *86*, 158.
(5) Dry, M. E. "Catalysis: Science and Technology"; Anderson, J. R., Boudart, M., Eds.; Springer-Verlag: Berlin, 1981; Vol. 1, Chapter 4.
(6) GC/MS analysis rather than simple mass spectroscopy was necessary because of the extensive fragmentation of olefins even at rather low electron energies.

0002-7863/85/1507-0696$01.50/0